

# Chiral phase transition with mixing between scalar quarkonium and tetraquark

Tamal K. Mukherjee<sup>1,2\*</sup> and Mei Huang<sup>1,2†</sup>

<sup>1</sup> *Institute of High Energy Physics, Chinese Academy of Sciences, Beijing, China*

<sup>2</sup> *Theoretical Physics Center for Science Facilities, Chinese Academy of Sciences, Beijing, China*

(Dated: February 16, 2019)

In the framework of two-flavor extended linear sigma model with mixing between scalar quarkonium and tetraquark, we investigate the role of the tetraquark in the chiral phase transition. We explore various scenarios depending on the value of various parameters in our model. The physical mass spectrum of mesons put a tight constraint on the parameter set of our model. We find a sufficiently strong cubic self interaction of the tetraquark field can drive the chiral phase transition to first order even at zero quark chemical potential. Weak or absence of the cubic self interaction term of the tetraquark field make the chiral phase transition crossover at vanishing density.

PACS numbers:

## I. INTRODUCTION

The role of chiral condensate is well known and well studied in the context of chiral phase transition. Recently, the possible role of tetraquark condensate in connection to the chiral phase transition is also being considered [1, 2]. The reason behind such consideration stems from the unsettled nature of the lightest scalar  $f_0(600)$  ( $f_0(500)$  in [3]) or  $\sigma$  meson. This issue is part of the unresolved nature of the scalar mesons below 2 GeV. There are about 19 scalar resonances found below 2 GeV which cannot be explained by the naive quark model. Their mass spectrum and decay patterns are also quite contrary to what is expected from the quark model. An intense effort is going on to understand the nature and properties of these mesons (see refs. [4–7] and references therein).

Theoretical understanding of the lightest scalar  $\sigma/f_0(600)$  is important as it is believed to be the Higgs Bosons of QCD and plays an important role in chiral symmetry breaking. Though its existence has been confirmed from the  $\pi\pi$  scattering process [5, 8], the consensus on its nature is still elusive. Conventionally  $f_0(600)$  is regarded as composed of quark-antiquark. But in order to solve the mass hierarchy problem for scalar mesons below 1 GeV, Jaffe [9] in 1977 proposed to consider the scalar meson below 1 GeV as tetraquark states and those above 1 GeV to be quarkonium dominated states. Thus, in this picture  $f_0(600)$  is predominantly a tetraquark states whereas  $f_0(1370)$  is the lightest quarkonium state made up of quark-antiquark. The sizable tetraquark component has also been demonstrated in a recent Lattice simulation study [10]. However, there are other suggestions as well, for example, recent data from  $\pi\pi$  and  $\gamma\gamma$  scattering [11, 12], the K-matrix analysis [13] suggests that it has sizable glueball content.

The role of chiral condensate as an order parameter for chiral phase transition is well established. But, the role of tetraquark condensate is not understood and work in this direction has recently been started [1, 2].

In [1] the implications of mixing between tetraquark and quarkonium fields on chiral phase transition is studied for zero baryon chemical potential. They favor the scenario where,  $f_0(600)$  is tetraquark dominated and the heavy  $f_0(1370)$  is quarkonium dominated. According to their study, the order of the phase transition is strongly correlated with the extent of mixing between the two fields. For a weak coupling constant for the mixing term, a soft first order phase transition is obtained. On the other hand for a strong coupling constant for the mixing term give rise to a crossover transition. Moreover, the most important and interesting result coming out from their study is that beyond a certain maximum temperature the nature of the heavy and lighter mesons is exchanged. The heavy  $f_0(1370)$  becomes tetraquark dominated and the lighter  $f_0(600)$  turns into quarkonium dominated and becomes degenerate with the pion after the chiral symmetry restoring phase transition.

Whereas in [2], an alternate breaking of chiral symmetry in dense matter was proposed. Using Ginzburg-Landau effective potential consisting of two and four quark states they show in dense matter a possible phase may arise where chiral symmetry is spontaneously broken but its center symmetry remains unbroken. In this phase conventional chiral condensate vanishes and the chiral symmetry breaking is due to the presence of quartic condensate. Finally chiral symmetry is restored as quartic condensate also vanishes. Existence of a tricritical point is also predicted between

---

\*Electronic address: mukherjee@ihep.ac.cn

†Electronic address: huangm@ihep.ac.cn

broken and unbroken center symmetric phase. Thus in this scenario, restoration of chiral symmetry occurs in two steps.

These studies warrant us to study the effect of mixing between the quarkonium and tetraquark condensates on the chiral phase transition in detail. Here in this work, we study two flavor chiral phase transition within the framework of extended linear sigma model taking into account both quarkonium and tetraquark effective fields. We fix parameters from the physical meson masses. Depending on the possible values of the various parameters, the resulting phase diagram is discussed.

The paper is organized as follows: in the next section we discuss about the model we are going to consider and how the various parameters in the model is fixed. In section III we present our result and finally we summarize and conclude in the last section.

## II. THE MODEL

We are going to investigate the effect of quarkonium and tetraquark mixing on chiral phase transition in the framework of quark-meson model. In this model, quarks propagate in the background potential of mesonic fields and interact with the vacuum expectation values of the scalar mean fields via Yukawa coupling. The generic form of the Lagrangian consist of a fermionic part ( $\mathcal{L}_q$ ) and a mesonic field part ( $\mathcal{L}_m$ ) and can be written as:

$$\begin{aligned}\mathcal{L} &= \mathcal{L}_q + \mathcal{L}_m \\ &= \bar{q}(i\gamma^\mu\partial_\mu - g_3\Phi - g_4\Phi')q + \mathcal{L}_m,\end{aligned}\tag{1}$$

with the mesonic part of the Lagrangian:

$$\begin{aligned}\mathcal{L}_m &= \text{Tr}(\partial_\mu\Phi\partial^\mu\Phi^\dagger) + \text{Tr}(\partial_\mu\Phi'\partial^\mu\Phi'^\dagger) - m_\Phi^2\text{Tr}(\Phi^\dagger\Phi) - m_{\Phi'}^2\text{Tr}(\Phi'^\dagger\Phi') \\ &\quad + \frac{\lambda_1}{2}\text{Tr}(\Phi^\dagger\Phi\Phi^\dagger\Phi) + \frac{\lambda_2}{2}\text{Tr}(\Phi'^\dagger\Phi'\Phi'^\dagger\Phi') \\ &\quad + g_2\text{Tr}(\Phi'\Phi'\Phi') - g_1\text{Tr}(\Phi')\text{Tr}(\Phi)\text{Tr}(\Phi) \\ &\quad + k[\text{Det}(\Phi) + h.c.] - h[\text{Tr}(\Phi) + h.c.].\end{aligned}\tag{2}$$

Where, for two light flavors the quark field "q" can be represented as  $q = (u, d)$  and  $g_3, g_4$  are the Yuakwa coupling constants for the quarkonium and tetraquark fields respectively. The mesonic Lagrangian part has two effective fields: a  $2 \times 2$  matrix field  $\Phi$  which denotes the bare quarkonium field and a  $2 \times 2$  matrix field  $\Phi'$  which denotes the bare tetraquark field. Following the convention of the linear sigma model, we express the quarkonium and the tetraquark fields as:

$$\Phi = \frac{1}{2}(\sigma_b + \eta_b) + \frac{1}{2}(\vec{\alpha}_b + i\vec{\pi}_b) \cdot \vec{\tau},\tag{3}$$

$$\Phi' = \frac{1}{2}(\sigma'_b + \eta'_b) + \frac{1}{2}(\vec{\alpha}'_b + i\vec{\pi}'_b) \cdot \vec{\tau},\tag{4}$$

with  $\tau_i$  ( $i = 1, 2, 3$ ) represents  $2 \times 2$  Pauli matrix. The transformation properties of these fields under  $U(2)_L \times U(2)_R$  symmetry are defined as follows:

$$\Phi \rightarrow U_L\Phi U_R^\dagger,\tag{5}$$

$$\Phi' \rightarrow U_L\Phi' U_R^\dagger,\tag{6}$$

where  $U_{L,R}$  are group elements of the  $U(2)_L \times U(2)_R$  symmetry.

The mesonic spectra consist of sixteen physical mesons: pair of scalar isoscalar  $\{f_0(600), f_0(1370)\}$ , pair of pseudoscalar isoscalar  $\{\eta_p, \eta'_p\}$ , pair of scalar isovector  $\{\vec{\alpha}_p, \vec{\alpha}'_p\}$  and pair of pseudoscalar isovector  $\{\vec{\pi}_p, \vec{\pi}'_p\}$ . Here, pseudoscalar isoscalar  $\eta_p$  and  $\eta'_p$  mesons are composed of  $u$  and  $d$  quarks only. The bare quarkonium and tetraquark fields mixed with each other to give rise to physical mesonic fields: one of them being quarkonium dominated and the other tetraquark dominated mesons.

In the mesonic part Lagrangian Eq.(2), the cubic term for the tetraquark meson has the coupling constant  $g_2$ , the mixing term between quarkonium and tetraquark has the coupling constant  $g_1$  and the last term mimicking the finite quark mass for the quarkonium with coupling constant  $h$  explicitly breaks the  $U(2)_L \times U(2)_R$  symmetry. Whereas, the instanton determinant term explicitly break the axial  $U(1)_A$  symmetry. The other terms in the potential part of the Lagrangian are invariant under  $U(2)_L \times U(2)_R$  symmetry. However, we spontaneously break the  $SU(2)_A$  part of the symmetry of these terms as well by assuming vacuum expectation values for the  $\sigma_b$  and  $\sigma'_b$  fields. The mass and the

quartic interaction terms are the standard terms used in the linear  $\sigma$  model. An explicit symmetry breaking term to account for the finite quark mass and an instanton determinant term for the field  $\Phi$  are also used. The explicit chiral symmetry breaking terms for the field  $\Phi$  renders  $\pi_b$  and  $\eta_b$  massive. The instanton determinant term is responsible for the splitting of masses between  $\pi_b$  and  $\eta_b$ . The choice of the cubic term is motivated from the study in ref. [2].

We will investigate the chiral phase transition at the mean field level. Following the standard procedure, we expand the fields around the vacuum expectation values:  $\sigma_b = \sigma + \sigma_f$  and  $\sigma'_b = \chi + \sigma'_f$ . Where,  $\sigma$  and  $\chi$  are the vacuum expectation values of the corresponding fields. Keeping only the mean fields and integrating out the fermionic fields we obtain the expression for the thermodynamical potential at temperature  $T$  and chemical potential  $\mu$  as:

$$\Omega = U(\sigma, \chi) - 2TN_c N_f \int \frac{d^3 q}{(2\pi)^3} [\ln(1 + e^{-(E_q - \mu)/T}) + \ln(1 + e^{-(E_q + \mu)/T})], \quad (7)$$

where

$$U(\sigma, \chi) = -\frac{1}{2}m_\Phi^2 \sigma^2 - \frac{1}{2}m_{\Phi'}^2 \chi^2 + \frac{1}{16}\lambda_1 \sigma^4 + \frac{1}{16}\lambda_2 \chi^4 + \frac{1}{4}g_2 \chi^3 - g_1 \sigma^2 \chi + \frac{1}{2}k\sigma^2 - 2h\sigma. \quad (8)$$

The single particle energy is given by  $E_q = \sqrt{p^2 + m_q^2}$  and the constituent quark mass ( $m_q$ ) is given by  $m_q = g_3\sigma + g_4\chi$ . The number of colours  $N_c$  and flavors  $N_f$  of quark used in this paper are 3 and 2 respectively.

From the extremum condition of the thermodynamic potential we obtain equation of motions for  $\sigma$  and  $\chi$ :

$$\frac{\partial \Omega}{\partial \sigma} = 0, \quad \frac{\partial \Omega}{\partial \chi} = 0. \quad (9)$$

We will solve this set of coupled equation of motions Eq.(9) self consistently at each values of temperature  $T$  and chemical potential  $\mu$  to determine the behavior of  $\sigma$  and  $\chi$  as a function of temperature and chemical potential, and analyze the effect of quarkonium-tetraquark mixing on the chiral phase transition.

### III. PARAMETER FIXING IN THE VACUUM

There are total 12 parameters in our model:  $m_\Phi^2$ ,  $m_{\Phi'}^2$ ,  $\lambda_1$ ,  $\lambda_2$ ,  $g_1$ ,  $g_2$ ,  $k$ ,  $h$ ,  $g_3$ ,  $g_4$  and zero temperature values of  $\sigma$ ,  $\chi$ . Out of these 12 parameters, the coupling constants  $g_3$ ,  $g_4$  are from the fermionic part ( $\mathcal{L}_q$ ) of the Lagrangian and the other 10 are from the mesonic part ( $\mathcal{L}_m$ ). The values of the 10 parameters in the mesonic part of the Lagrangian are determined from the physical meson masses, the pion decay constant ( $f_\pi = 92.4$  MeV) and two extremum conditions for the mesonic potential:

$$\frac{\partial U(\sigma, \chi)}{\partial \sigma} = 0, \quad \frac{\partial U(\sigma, \chi)}{\partial \chi} = 0. \quad (10)$$

Values of the parameters so fixed are kept constant for the whole range of temperature and chemical potential. The physical meson masses are so chosen that for each kind of meson, one of the mass is below 1GeV and the other is above 1GeV. One of them is likely choice for the quarkonium dominated meson and the other is tetraquark dominated as found by other studies [14, 15].

The physical meson masses are obtained by diagonalizing the bare meson mass matrices. The expression for those bare matrices as a function of quarkonium, tetraquark fields and the coupling constants, are noted below:

For the sigma mesons we have:

$$(M_{f_0}^2) = \begin{bmatrix} \frac{1}{2}\lambda_1 \sigma^2 + 2\frac{h}{\sigma} & -2g_1 \sigma \\ -2g_1 \sigma & \frac{1}{2}\lambda_2 \chi^2 + \frac{3}{4}g_2 \chi + g_1 \frac{\sigma^2}{\chi} \end{bmatrix}. \quad (11)$$

For pions we have:

$$(M_\pi^2) = \begin{bmatrix} 2g_1 \chi + 2\frac{h}{\sigma} & 0 \\ 0 & g_1 \frac{\sigma^2}{\chi} - \frac{9}{4}g_2 \chi \end{bmatrix}. \quad (12)$$

For eta we have,

$$(M_\eta^2) = \begin{bmatrix} 4g_1\chi - 2k + 2\frac{h}{\sigma} & 2g_1\sigma \\ 2g_1\sigma & -\frac{9}{4}g_2\chi + g_1\frac{\sigma^2}{\chi} \end{bmatrix}. \quad (13)$$

Lastly bare mass matrix for the  $\alpha_p$  meson reads,

$$(M_\alpha^2) = \begin{bmatrix} \frac{1}{2}\lambda_1\sigma^2 + 2\frac{h}{\sigma} + 2g_1\chi - 2k & 0 \\ 0 & \frac{1}{2}\lambda_2\chi^2 + \frac{3}{4}g_2\chi + g_1\frac{\sigma^2}{\chi} \end{bmatrix}. \quad (14)$$

From the mass matrices, we find that there is no mixing for the pion and  $\alpha$  mesons. We choose the lightest pion as a quarkonium meson and the heavier counterpart as tetraquark meson in its quark content. This is in agreement with our current understanding. Since there is no mixing for pion, we define the zero temperature value of  $\sigma$  equal to the pion decay constant ( $\sigma = f_\pi$ ). From the expression of pion mass we see the symmetry breaking terms contribute towards its mass and the absence of those terms in our Lagrangian would make pion massless. The same statement is also holds for the eta mesons although in this case there is mixing between quarkonium and tetraquark fields. In absence of mixing,  $(M_\eta^2)_{11}$  would represent the physical eta meson mass and comparing it with conventional pion mass  $(M_\pi^2)_{11}$  we find the difference between their masses are coming from the instanton term, which is in line with our expectation.

In the following, we discuss three sets of parameters, which will be used for our analysis of chiral phase transition in Sec.IV.

#### A. Case I: $\lambda_2, g_2, k, h = 0$

In this case, the values of the parameters  $\lambda_1, g_1$  and the zero temperature value of  $\chi$  are calculated using the physical masses of  $m_{f_0(600)}, m_{f_0(1370)}, m_{\pi_p}, m_{\pi'_p}$  mesons and the values of  $m_\Phi^2, m_{\Phi'}^2$  are calculated using the extremum conditions for mesonic potential (see eqn. (10)). Please note that even if  $h = 0$  in this case, the  $\pi_p$  meson is still massive because of the interaction term between quarkonium and tetraquark fields which breaks the chiral symmetry explicitly. Utilizing the expressions for  $\pi_p$  and  $\pi'_p$  masses together with the relations:

$$\text{Tr}[(M_{f_0}^2)] = m_{f_0(600)}^2 + m_{f_0(1370)}^2, \quad (15)$$

$$\text{Det}[(M_{f_0}^2)] = m_{f_0(600)}^2 \times m_{f_0(1370)}^2, \quad (16)$$

we get the expressions for  $g_1, \chi, \lambda_1$  as:

$$g_1 = \frac{1}{2f_\pi} \sqrt{(m_{f_0(600)}^2 + m_{f_0(1370)}^2 - m_{\pi'_p}^2) m_{\pi'_p}^2 - m_{f_0(600)}^2 \times m_{f_0(1370)}^2}, \quad (17)$$

$$\chi = g_1 \frac{\sigma^2}{m_{\pi'_p}^2}, \quad (18)$$

$$\lambda_1 = \frac{2}{\sigma^2} [m_{f_0(600)}^2 + m_{f_0(1370)}^2 - m_{\pi'_p}^2]. \quad (19)$$

Using Eq. (10), we can calculate the values for  $m_\Phi^2$  and  $m_{\Phi'}^2$  from the expressions:

$$m_\Phi^2 = -\left(-\frac{1}{4}\lambda_1\sigma^2 + 2g_1\chi\right), \quad (20)$$

$$m_{\Phi'}^2 = -g_1 \frac{\sigma^2}{\chi}. \quad (21)$$

The values of the physical meson masses used is given in table I. Depending on what value we choose for the mass of  $m_{\pi'_p}$ , we get two scenarios:

Scenario 1: The values of the parameter are such that the lowest scalar  $f_0(600)$  is a quarkonium dominated meson, whereas the heavier one  $f_0(1370)$  is tetraquark dominated. The values of the parameters are given in table II.

Scenario 2: In this case the nature of the scalar isoscalar mesons are just opposite to that of Scenario 1. But for that we have to take the input values for  $m_{\pi'_p}$  slightly less than its range of possible values 1.2 – 1.4 GeV. Here, the lowest scalar  $f_0(600)$  is a tetraquark dominated meson, whereas the heavier one  $f_0(1370)$  is quarkonium dominated. The values of the parameters so obtained are given in table II.

Mesons	$m_{f_0(600)}$ (GeV)	$m_{f_0(1370)}$ (GeV)	$m_{\pi_p}$ (GeV)	$m_{\pi'_p}$ (GeV)
Scenario 1	0.8	1.5	0.14	1.3
Scenario 2	0.8	1.5	0.14	1.1

TABLE I: Values of physical meson masses used in Case I.

Parameters	$\sigma$ (GeV)	$\chi$ (GeV)	$m_\Phi^2$ (GeV <sup>2</sup> )	$m_{\Phi'}^2$ (GeV <sup>2</sup> )	$\lambda_1$	$g_1$ (GeV)
Scenario 1	0.0924	0.021	0.426	-1.69	281.1	4.15
Scenario 2	0.0924	0.029	0.595	-1.21	393.55	4.17

TABLE II: Parameter set for Case I.

### B. Case II: $\lambda_2, k, h \neq 0$ but $g_2 = 0$

To discuss how the parameter set for  $g_2 = 0$  is obtained, we first write down the equations we are going to use to determine the values of  $g_1$ ,  $\chi$ ,  $h$  and  $k$ ,

$$m_{\pi_p}^2 = 2 g_1 \chi + 2 \frac{h}{\sigma}, \quad (22)$$

$$m_{\pi'_p}^2 = g_1 \frac{\sigma^2}{\chi}, \quad (23)$$

$$\text{Tr} [(M_\eta^2)] = m_{\eta_p}^2 + m_{\eta'_p}^2, \quad (24)$$

$$\text{Det} [(M_\eta^2)] = m_{\eta_p}^2 \times m_{\eta'_p}^2. \quad (25)$$

Now, utilizing equations (23), (24) and (25) we get the equation for  $g_1$  as:

$$g_1 = \frac{1}{2\sigma} \sqrt{(m_{\eta_p}^2 + m_{\eta'_p}^2 - m_{\pi_p}^2) m_{\pi'_p}^2 - m_{\eta_p}^2 \times m_{\eta'_p}^2} \quad (26)$$

From (23), we get the chiral condensate as,

$$\chi = g_1 \frac{\sigma^2}{m_{\pi'_p}^2}. \quad (27)$$

Using (22), (26) and (27) we can determine the value of  $h$  from the following equation,

$$h = \frac{\sigma}{2} [m_{\pi_p}^2 - 2 g_1 \chi]. \quad (28)$$

According to convention followed in this paper the vacuum expectation values:  $\sigma$  and  $\chi$  are positive. To make sure we have the minimum of the mesonic potential lie in the quadrant where both  $\sigma$  and  $\chi$  are positive, we should have  $g_1 > 0$  and  $h > 0$ . Apart from that we should also have positive  $\lambda_1$ ,  $\lambda_2$  in order to make our mesonic potential bounded from below. There is a large uncertainties in the value of  $m_{\pi'_p}$  - (1.2 – 1.4)GeV. But if we impose the constraints  $g_1 > 0$  and  $h > 0$  and fix the values of  $m_{\eta_p}$  and  $m_{\eta'_p}$  at 0.55 and 1.3GeV respectively, we find only allowed value is  $m_{\pi'_p} = 1.29\text{GeV}$  (up to two significant digits after decimal). Mass values higher than that would make  $g_1 < 0$  and for mass less than 1.29GeV the value of  $h$  becomes negative.

The value of  $k$  can be determined from (22), (23) and (24),

$$k = \frac{1}{2} [2 g_1 \chi - (m_{\eta_p}^2 + m_{\eta'_p}^2 - m_{\pi_p}^2 - m_{\pi'_p}^2)] \quad (29)$$

Then the mass matrix of  $f_0$  mesons can be utilized to determine the values of  $\lambda_1$  and  $\lambda_2$ . The relevant equations here are:

$$\text{Tr} [(M_{f_0}^2)] = m_{f_0(600)}^2 + m_{f_0(1370)}^2, \quad (30)$$

$$\text{Det} [(M_{f_0}^2)] = m_{f_0(600)}^2 \times m_{f_0(1370)}^2. \quad (31)$$

Like the value of  $m_{\pi'_p}$ , there are also large uncertainties in the values of  $m_{f_0(600)}$ :  $(0.4 - 1.2)\text{GeV}$  and  $m_{f_0(1370)}$ :  $(1.2 - 1.5)\text{GeV}$ . Here we have used,  $m_{f_0(600)} = 0.6\text{GeV}$  and  $m_{f_0(1370)} = 1.35\text{GeV}$ . Two sets of values can be obtained from equations (30) and (31). But only one of them satisfies the condition:  $\lambda_1, \lambda_2 > 0$  and considered in this work. We have checked for other values of  $m_{f_0(600)}$  in the range  $(0.4 - 1.2)\text{GeV}$  and  $m_{f_0(1370)}$  in the range  $(1.2 - 1.5)\text{GeV}$  and one of the solution for  $\lambda_2$  remains always negative for the entire mass range.

Finally the values of  $m_{\Phi}^2$  and  $m_{\Phi'}^2$  can be determined from the extremum condition mentioned in Eq. (10). The explicit expression for them is given below:

$$m_{\Phi}^2 = - \left( -\frac{1}{4} \lambda_1 \sigma^2 + 2 g_1 \chi - k + 2 \frac{h}{\sigma} \right), \quad (32)$$

$$m_{\Phi'}^2 = - \left( -\frac{1}{4} \lambda_2 \chi^2 + g_1 \frac{\sigma^2}{\chi} \right). \quad (33)$$

The values of the input physical meson masses and the resultant output parameter set are given in Table III and Table IV respectively.

Fields	$m_{f_0(600)}$	$m_{f_0(1370)}$	$m_{\pi_p}$	$m_{\pi'_p}$	$m_{\eta_p}$	$m_{\eta'_p}$
Mass (GeV)	0.6	1.35	0.14	1.29	0.55	1.3

TABLE III: Value of physical meson masses used for case II.

Parameters	$\sigma$ (GeV)	$\chi$ (GeV)	$m_{\Phi}^2$ (GeV <sup>2</sup> )	$m_{\Phi'}^2$ (GeV <sup>2</sup> )	$\lambda_1$	$\lambda_2$	$g_1$ (GeV)	$h$ (GeV <sup>3</sup> )	$k$ (GeV <sup>2</sup> )
Value	0.0924	0.00523	0.019	-1.6	87.99	9103.07	1.02	0.00042	-0.149

TABLE IV: Parameter set for case II.

### C. Case III: $\lambda_2, g_2, k, h \neq 0$

To fix the parameters for  $g_2 \neq 0$  we follow the same procedure as mentioned above. Here in this case we have one more parameter  $g_2$ . For this, we made an assumption that  $\chi < \sigma$ , which holds good for all previous studies. Now the constraints,  $g_1 > 0$ ,  $h > 0$ ,  $\lambda_1 > 0$ ,  $\lambda_2 > 0$  restrict the value of  $\chi$  to a certain range. We assume  $\chi = \sigma/n$  and calculate the parameter set for small and large possible values of "n" ( $n = 10$  and  $18$ ) respecting all the constraints.

The expressions for  $g_1$ ,  $h$ ,  $k$  remains the same as mentioned in Eqs. (26), (28) and (29). The expression for  $g_2$  in this case reads as follows:

$$g_2 = \frac{4}{9\chi} \left( g_1 \frac{\sigma^2}{\chi} - m_{\pi'_p}^2 \right). \quad (34)$$

Here for  $n = 10$ , i.e., if  $\chi$  is small, we get the sign of  $g_2$  to be positive. While for  $n = 18$ , corresponding to comparatively large value of  $\chi$ , the sign of  $g_2$  becomes negative. The values of  $\lambda_1$  and  $\lambda_2$  are calculated using Eqs. (30) and (31).

Finally  $m_{\Phi}^2$  and  $m_{\Phi'}^2$  are calculated from the following expressions using Eq. (10):

$$m_{\Phi}^2 = - \left( -\frac{1}{4} \lambda_1 \sigma^2 + 2 g_1 \chi - k + 2 \frac{h}{\sigma} \right) \quad (35)$$

$$m_{\Phi'}^2 = - \left( -\frac{1}{4} \lambda_2 \chi^2 + g_1 \frac{\sigma^2}{\chi} - \frac{3}{4} g_2 \chi \right) \quad (36)$$

As in the case for  $g_2 = 0$ , here also, we only find one set of solution which respect the constrain  $\lambda_1 > 0$  and  $\lambda_2 > 0$ . The values of the input physical meson masses used here are the same as in the previous section (see Table III) and the output parameters obtained are given in Table V and VI corresponding to positive and negative  $g_2$  respectively.

Parameters	$\sigma$ (GeV)	$\chi$ (GeV)	$m_\Phi^2$ (GeV <sup>2</sup> )	$m_{\Phi'}^2$ (GeV <sup>2</sup> )	$\lambda_1$	$\lambda_2$	$g_1$ (GeV)	$g_2$ (GeV)	$h$ (GeV <sup>3</sup> )	$k$ (GeV <sup>2</sup> )
Value	0.0924	0.00513	0.019	-1.63	87.93	7527.9	1.016	2.25	0.00042	-0.149

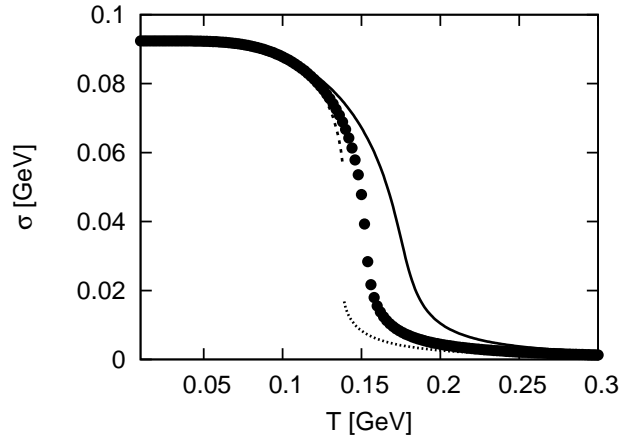
TABLE V: Parameter set for  $g_2 \neq 0$ . In this set,  $\chi = \sigma/n$  where  $n = 18$  is used.

Parameters	$\sigma$ (GeV)	$\chi$ (GeV)	$m_\Phi^2$ (GeV <sup>2</sup> )	$m_{\Phi'}^2$ (GeV <sup>2</sup> )	$\lambda_1$	$\lambda_2$	$g_1$ (GeV)	$g_2$ (GeV)	$h$ (GeV <sup>3</sup> )	$k$ (GeV <sup>2</sup> )
Value	0.0924	0.00924	0.027	-0.63	89.88	25785.1	1.02	-34.88	0.000038	-0.145

TABLE VI: Parameter set for  $g_2 \neq 0$ . In this set,  $\chi = \sigma/n$  where  $n = 10$  is used.

#### IV. RESULTS FOR PHASE TRANSITIONS

There are two more parameters in our model which are not discussed yet. They are the Yukawa coupling constants  $g_3$  and  $g_4$ . Their values are fixed from the given value of the constituent quark mass. Since we have one condition and two undetermined coupling constants, we assume,  $g_4 = g_3/n_\chi$  where  $n_\chi > 1$ . For a particular value of  $g_3$  if we change the value of  $g_4$  by changing  $n_\chi$  then there is no qualitative change in the behaviour of  $\sigma$ ,  $\chi$ . However, nature of phase transition is affected if we change the value of  $g_3$ . This can be seen from Fig. 1. If we increase the value of  $g_3$  then we can get first order transition even at zero chemical potential. This dependence of the order of the phase transition on the values of the model parameters in mean field approximation of Linear Sigma Model/Quark Meson Model is not new and already noted in [1, 16, 17]. In this work, we have used  $g_3 = 3.0$  and  $g_4 = g_3/10$  corresponding to vacuum constituent quark mass of 0.28 GeV. This values is chosen to make the chiral phase transition crossover at zero chemical potential, as found by Lattice simulation study [18].

FIG. 1: Variation of  $\sigma$  with temperature at zero chemical potential for different values of  $g_3$ . From left to right the values of  $g_3$  are 3.5, 3.0 and 2.5. Parameters are corresponding to the scenario  $g_2 = 0$ , i.e., Table IV.

Before presenting our result, let us first discuss the nature of the mesonic potential  $U(\sigma, \chi)$  in vacuum. As can be seen from the parameter set presented in Table IV, V, VI, the sign of  $m_{\Phi'}^2$  is opposite to that of  $m_\Phi^2$ . Its sign indicates that it has opposite sign to what requires for spontaneous breaking. This can be seen from the figure 2 (right one) where the potential in the  $\chi$  direction (for constant  $\sigma = 0.0924$  GeV) is plotted. There is only one minimum and the minimum of the potential is slightly tilted in the  $\chi > 0$  direction because of the explicit symmetry breaking terms. On the other hand because of the negative sign of  $m_\Phi^2$ , the potential in the  $\sigma$  direction exhibits the kind of pattern expected for spontaneous symmetry breaking. The minima in the  $\sigma > 0$  direction is lower than that in the opposite direction (see left hand figure of 2, here  $\chi = 0.00523$  GeV) because of  $h > 0$ . Thus the origin of  $\sigma$  and  $\chi$  condensates have different reasons in this work. Explicit symmetry breaking is the origin for  $\chi$ , whereas for  $\sigma$  it is

the spontaneous breaking.

For values of parameters presented in Tables IV, V and VI, we find, irrespective of the scalar or pseudoscalar nature of the mesons, mesons with lower mass is always quarkonium dominated and the mesons above 1 GeV is tetraquark dominated. The mixing angle for  $f_0$  meson for parameter sets presented in Tables IV, V and VI is -7.51, -7.44 and -7.45 (in degrees) respectively. For  $\eta$  mesons the mixing angle for the above mentioned parameter sets is 7.88, 7.84 and 7.86 (in degrees) respectively. Like pions, there is no mixing for  $\alpha$  meson. The masses of  $\alpha_p$ ,  $\alpha'_p$  mesons are 0.83 and 1.34 GeV respectively for all three parameter sets. Since there is no mixing, the lower mass  $\alpha_p$  meson is purely quarkonium and the heavier counterpart is purely tetraquark in nature.

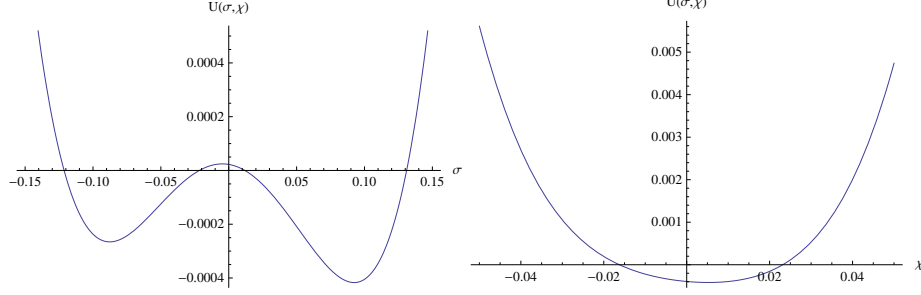


FIG. 2: Nature of the mesonic potential  $U(\sigma, \chi)$  in vacuum. Parameters are corresponding to table IV. See text for details.

To characterize the phase transition and to find the transition temperature we have used the susceptibilities of the order parameters. The susceptibility matrix is defined as [2, 19];

$$\hat{\chi} = \frac{1}{C_{\chi\chi} C_{\sigma\sigma} - C_{\sigma\chi}^2} \begin{bmatrix} C_{\chi\chi} & C_{\sigma\chi} \\ C_{\sigma\chi} & C_{\sigma\sigma} \end{bmatrix}. \quad (37)$$

Where  $C_{xx}$  ( $x = \sigma, \chi$ ) are the second derivative of the thermodynamic potential w.r.t  $x$ :

$$C_{xx} = \frac{\partial^2 \Omega}{\partial x^2}. \quad (38)$$

Susceptibility of  $\sigma$  is defined as  $\chi_{2Q} = \hat{\chi}_{11}$  and that of  $\chi$  is given by  $\chi_{4Q} = \hat{\chi}_{22}$ . We determine the transition temperature from the peak position of the respective susceptibilities. For critical point,  $C_{\chi\chi} C_{\sigma\sigma} - C_{\sigma\chi}^2$  becomes zero corresponding to zero curvature of the thermodynamic potential.

### A. Phase diagram for Case I

The behaviour of the order parameters along with the resultant phase diagram corresponding to the parameter set for Case I are summarized in Figs. 3, 4.

As mentioned in the last section, here we have two scenarios depending on the mass of  $m_{\pi'}$ . For  $m_{\pi'} = 1.3$  GeV corresponding to scenario 1, the lowest isoscalar is quarkonium dominated. Whereas, for scenario 2, we consider  $m_{\pi'} = 1.1$  GeV (which is slightly less than the value quoted in the Particle data group: 1.2-1.4 GeV), we have lowest isoscalar as tetraquark dominated meson.

We find, for both the cases for all values of the chemical potential the transition temperatures calculated from the susceptibilities  $\chi_{2Q}$  and  $\chi_{4Q}$  are the same. This can also be seen from the behaviour of the order parameters presented in Fig. 3. In Fig. 3, the temperature variation of  $\sigma$  and  $\chi$  are presented for low and high values of chemical potential. From the figure, we see  $\sigma$  and  $\chi$  varies more slowly with temperature in the case for scenario 2 than in scenario 1. Consequently, the transition temperature in scenario 2 is always higher than the scenario 1. For both the scenarios, both  $\sigma$  and  $\chi$  goes to zero after the phase transition because of  $h = 0$ . But for scenario 1, there is a jump in case of  $\sigma$  after a certain temperature and this gap in the order parameter increases slowly with the chemical potential. For  $\chi$ , this gap is vanishingly small at low chemical potential and slowly increases with the chemical potential.

If we compare the phase diagrams shown in Fig. (4), we see for scenario 2, the order of the phase transition is second order both for low as well as high values of the chemical potential. But for scenario 1, the second order of



phase transition changes to weak first order phase transition above some critical value of the chemical potential, thus indicates presence of a critical point. We consider the values of the chemical potential and temperature at which the curvature of the thermodynamic potential becomes greater than  $10^{-4}$ , as the location of the critical point. Using this condition, we find the critical point for scenario 1 is located at  $T_c = 117.7$  MeV and  $\mu_c = 335$  MeV. The departure from the zero curvature of the thermodynamical potential together with the gap in the order parameter are taken as the indication of weak first order phase transition. We are calling it weak first order because curvature of the thermodynamic potential remains very small ( $10^{-3}$ ) for  $\mu > 335$  MeV.

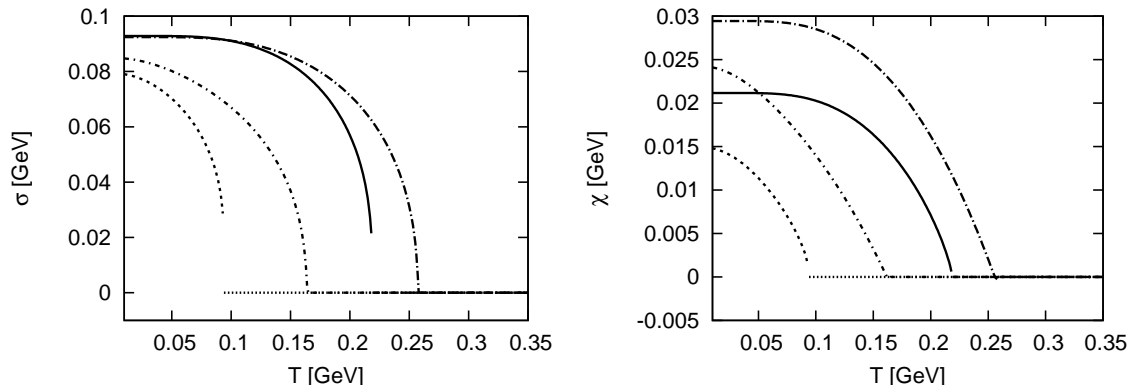


FIG. 3: Variation of  $\sigma$  and  $\chi$  with temperature for different values of chemical potential corresponding to parameter set of Case I. The solid ( $\mu = 0$  GeV) and dotted ( $\mu = 0.36$  GeV) lines are for scenario 1. Whereas, the long ( $\mu = 0.0$  GeV) and short dash-dot ( $\mu = 0.36$  GeV) lines are for scenario 2.

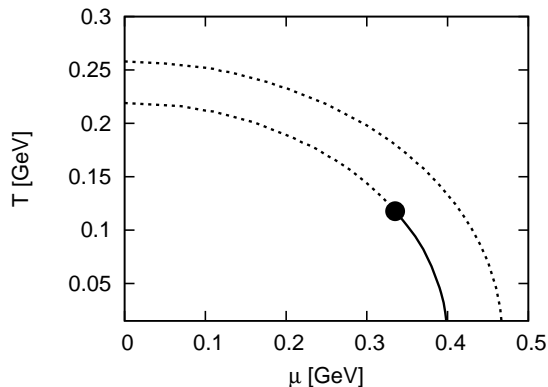


FIG. 4: Phase diagram for Case I. The dotted line represents second order phase transition and the solid line stands for first order phase transition. The upper phase boundary line corresponds to scenario 2 and the lower one corresponds to scenario 1.

### B. Phase diagram for Case II and Case III

The nature of the phase transition corresponding to Case II and III are summarized in Figs. 5 and 6.

Behaviour of the order parameters at low and high values of the chemical potentials are presented in Fig. 5, where the left figure corresponds to  $g_2 = 0$  and the right one  $g_2 < 0$ . We find for  $g_2 = 0$  (see Table IV) and  $g_2 > 0$  (see table VI) the behaviour of the order parameters are qualitatively similar. This is expected as the positive cubic

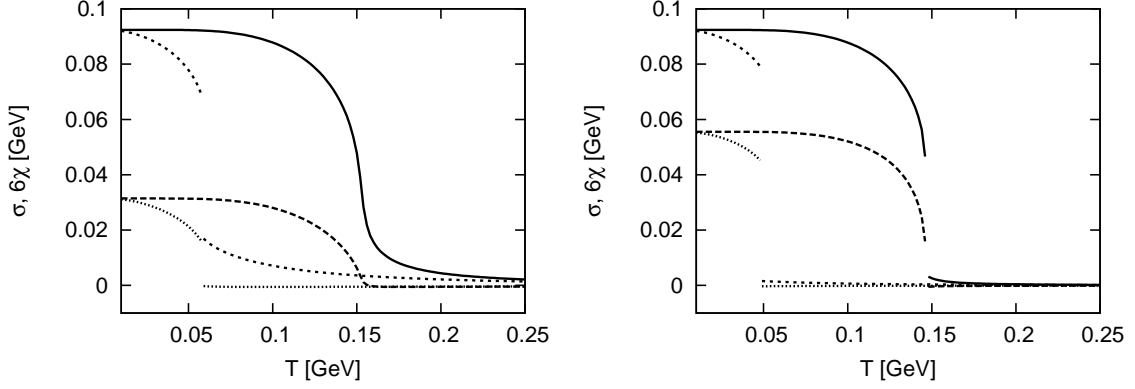


FIG. 5: Variation of  $\sigma$  and  $\chi$  with temperature for different values of chemical potential. Figure in the left panel is for  $g_2 = 0$  and the right one is for  $g_2 = -34.88$ . The solid ( $\mu = 0$  GeV) and short dash ( $\mu = 0.27$  GeV) lines are for variation of  $\sigma$ . Variation of  $\chi$  is represented by long dash ( $\mu = 0$  GeV) and points ( $\mu = 0.27$  GeV) for both the figures.

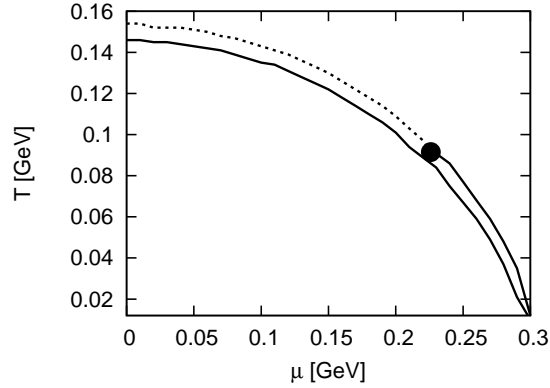


FIG. 6: Phase diagram for Case III. The solid line indicates first order phase transition and the dashed line is for crossover transition. The upper phase boundary is for  $g_2 = 2.25$  and the lower one is for  $g_2 = -34.88$ . The bold circle indicates location of the critical end point. See text for details

interaction coupling constant is relatively small and the other parameters being almost of same values. As can be seen from Fig. 5 (left), for small chemical potential we have a crossover transition which turns into first order transition at high value of the chemical potential. Because of finite " $h$ " term for the  $\Phi$  field makes  $\sigma > 0$  even at high temperature. But absence of such term for the  $\Phi'$  field makes  $\chi$  goes to zero at high temperature. However, the nature of the transition is quite different corresponding to scenario  $g_2 < 0$  (see Table V). In this case, the strong cubic interaction term make the transition first order for the whole range of chemical potential as can be seen from Fig. 5 (right). Here relatively low value of " $h$ " makes  $\sigma$  goes to zero at high temperature. However, there is one similarity with respect to chiral phase transition temperature for various cases considered in this work. Like Case I, we note from both the figures in Fig. 5, the transition for  $\sigma$  and  $\chi$  are occurring at the same temperature which is verified from the peak positions of the respective susceptibilities.

As a result, the resultant phase diagram shown in Fig. 6 is represented with a single phase boundary line for each case. For  $g_2 = 0$  and  $g_2 > 0$  we have qualitatively same feature and thus we have included the phase boundary for  $g_2 > 0$  only in Fig. 6. In this case, we have a crossover transition at low chemical potential which turns into first order above some critical value of the chemical potential. Thus, we have a critical end point for  $g_2 = 0$  and  $g_2 > 0$ . The location of the critical end point for  $g_2 = 0$  is ( $\mu = 0.26$  GeV,  $T = 0.069$  GeV) and for  $g_2 > 0$  is ( $\mu = 0.226$  GeV,

$T = 0.0915$  GeV). Whereas, for  $g_2 < 0$  we have only first order phase transition line owing to strong cubic interaction term.

## V. SUMMARY AND CONCLUSION

In the framework of two flavor quark-meson model, we have investigated the effect of mixing between quarkonium and tetraquark fields on chiral phase transition.

The mixing between the effective fields is introduced through an interaction term which breaks the chiral symmetry explicitly. In addition to the interaction term, we also considered a cubic self interaction term for the effective tetraquark field, an instanton determinant term and a term mimicking the effect of current quark mass. The parameters of our model is calculated from the masses of the physical mesons, pion decay constants and the stability conditions of the mesonic potential. We first considered the effect of the mixing term without considering the cubic self interaction term for the tetraquark field, the term mimicking the current quark mass and the instanton determinant term. Within the allowed experimental range for the masses for  $f_0(600)$ ,  $f_0(1370)$ ,  $\pi$  and  $\pi'$  mesons we find our lowest scalar  $f_0(600)$  meson is quarkonium dominated. Whereas, if we lower the mass of the  $\pi'$  meson we can have  $f_0(600)$  to be tetraquark dominated meson. The mass of the bare tetraquark field ( $\Phi'$ ) is strongly correlated with the  $\pi'$  mass and its value is equal to the negative of the  $\pi'$  mass.

For the scenario where  $f_0(600)$  is tetraquark dominated, we find the chiral phase transition is second order for both low and high values of the quark chemical potential. On the other hand, if we increase the absolute value of the mass of the bare tetraquark field, thereby increasing the value of the  $\pi'$  mass, we can have a weak first order phase transition above some critical value of the chemical potential. Comparing the transition in both cases, we find transition temperature is lowered with the increase of the absolute value of bare tetraquark field mass.

Next we study the effect of the cubic self interaction term (with coupling constant  $g_2$ ) of the tetraquark fields. We find physical meson mass spectrum and the vacuum stability conditions put a tight constraint on our parameter set. From the resulting parameter sets, we find lowest scalar meson  $f_0(600)$  is a quarkonium dominated meson whereas,  $f_0(1370)$  is tetraquark dominated. For  $g_2 = 0$  (but including the effect of finite current quark mass and the instanton term) and small but positive  $g_2$ , the chiral phase transition is crossover for small values of the quark chemical potential and then above some critical value of the chemical potential the transition becomes first order. Thus we have a critical end point in this case and the resultant phase diagram matches well with current consensus regarding the two flavor phase diagram. But with a strong and negative  $g_2$  makes not only the transition of  $\chi$  first order but the transition for  $\sigma$  as well becomes first order irrespective of the low or high value of the quark chemical potential. The strong and negative  $g_2$  also makes the chiral phase transition temperature lowered than that for the case of  $g_2 = 0$  or positive. For all the various scenarios considered in our study, the common feature among all of them is that the transition for quarkonium and tetraquark happening at the same temperature for all values of the chemical potential.

## Acknowledgments:

This work is supported by the NSFC under Grants No. 11250110058 and No. 11275213, DFG and NSFC (CRC 110), CAS fellowship for young foreign scientists under Grant No. 2011Y2JB05, CAS key project KJCX2-EW-N01, K.C.Wong Education Foundation and Youth Innovation Promotion Association of CAS.

- 
- [1] A. Heinz, S. Struber, F. Giacosa, D. H. Rischke, Phys. Rev. **D 79**, 037502 (2009).
  - [2] M. Harada, C. Sasaki, S. Takemoto. Phys. Rev. **D 81**, 016009 (2010).
  - [3] F. J. Yndurain, R. Garcia-Martin and J. R. Pelaez, Phys. Rev. **D 76**, 074034 (2007) [hep-ph/0701025]; J. R. Pelaez, J. Nebreda, G. Ros and J. Ruiz de Elvira, arXiv:1304.5121 [hep-ph]; J. R. Pelaez, PoS CD **12**, 047 (2013), [arXiv:1303.0125 [hep-ph]].
  - [4] K. Nakamura et al. (Particle Data Group), J. Phys. **G 37**, 075021 (2010).
  - [5] K. F. Liu, arXiv:0805.3364 [hep-lat]; K. F. Liu and C. W. Wong, Phys. Lett. **B 107**, 391 (1981); H. Y. Cheng, C. K. Chua and K. F. Liu, Phys. Rev. **D 74**, 094005 (2006); G. 't. Hooft, G. Isidori, L. Maiani, A. D. Polosa and V. Riquer, Phys. Lett. **B 662**, 424 (2008); Q. Zhao, B. S. Zou and Z. B. Ma, Phys. Lett. **B 631**, 22 (2005); D. V. Bugg, M. J. Peardon and B. S. Zou, Phys. Lett. **B 486**, 49 (2000).
  - [6] S. Narison, Nucl. Phys. Proc. Suppl. **186**, 306 (2009)
  - [7] V. Mathieu, N. Kochelev and V. Vento, Int. J. Mod. Phys. **E 18**, 1 (2009); E. Klempt and A. Zaitsev, Phys. Rept. **454**, 1 (2007); C. Amsler and N. A. Tornqvist, Phys. Rept. **389**, 61 (2004).
  - [8] I. Caprini, G. Colangelo and H. Leutwyler, Phys. Rev. Lett. **96**, 132001 (2006) [hep-ph/0512364].
  - [9] R. L. Jaffe, Phys. Rev. **D15**, 267, 1977.

- [10] S. Prelovsek, T. Draper, C. B. Lang, M. Limmer, K. -F. Liu, N. Mathur and D. Mohler, Phys. Rev. D **82**, 094507 (2010) [arXiv:1005.0948 [hep-lat]].
- [11] P. Minkowski and W. Ochs, Eur. Phys. J. C **9**, 283 (1999) [hep-ph/9811518].
- [12] G. Mennessier, S. Narison and W. Ochs, Phys. Lett. B **665**, 205 (2008) [arXiv:0804.4452 [hep-ph]].
- [13] G. Mennessier, S. Narison and X. G. Wang, Phys. Lett. B **688**, 59 (2010) [arXiv:1002.1402 [hep-ph]].
- [14] A. H. Fariborz, R. Jora, J. Schechter, Phys. Rev. D **79**, 074014 (2009).
- [15] T. K. Mukherjee, M. Huang, Q. S. Yan, Phys. Rev. D **86**, 114022 (2012).
- [16] A. Mocsy, Phys. Rev. D **66**, 056010 (2002).
- [17] B. J. Schaefer, J. Wambach, Phys. Rev. D **75**, 085015 (2007).
- [18] Z. Fodor, S. D. Katz, JHEP **0404**, 050 (2004).
- [19] C. Sasaki, B. Friman, K. Redlich, Phys. Rev. D **75**, 074013 (2007).